Materials Research Proceedings **25** (2023) 379-386 https://doi.org/10.21741/9781644902417-47

Evaluating material failure of AHSS using acoustic emission analysis

Eugen Stockburger[1,a,*], Hendrik Vogt[1,b], Hendrik Wester[1,c], Sven Hübner[1,d], and Bernd-Arno Behrens[1,e]

[1]Institut für Umformtechnik und Umformmaschinen, Leibniz Universität Hannover, An der Universität 2, 30823 Garbsen, Germany

[a]stockburger@ifum.uni-hannover.de, [b]vogt@ifum.uni-hannover.de, [c]wester@ifum.uni-hannover.de, [d]huebner@ifum.uni-hannover.de, [e]behrens@ifum.uni-hannover.de

*Corresponding author

Keywords: Fracture Analysis, High Strength Steel, Acoustic Emission

Abstract. Driven by high energy prices and strict legal requirements on CO_2 emissions, high-strength sheet steel materials are increasingly gaining importance in the automotive industry regarding electric vehicles and their battery range. Simulation-based design of forming processes can contribute to exploiting their high potential for lightweight design. However, previous studies show that numerical simulation with conventional forming limit curves does not always provide adequate prediction quality. Failure models that take the stress state into account represent an alternative prediction method for the shear-dominated failure, that frequently occur in high-strength steels during forming. The failure behaviour of the sheet materials can be determined by different specimen geometries for a wide range of stress states and by using an optical measurement system to record the local strain on the surface of the specimen at the location of failure. However, for many high-strength steels, critical damage or failure initiation already occurs inside the specimen. Therefore, a method is needed that allows detection of failure initiation at an early stage before the crack becomes visible on the surface of the specimen. One possible method is the use of acoustic emission analysis. By coupling it with an imaging technique, the critical strains leading to failure initiation inside the specimen can be determined. In the presented paper, butterfly tests are performed for a wide range of stress states and measured with an optical as well as an acoustical measurement system. The tests are analysed regarding the failure initiation using a mechanical, optical as well as acoustical evaluation method and compared with each other.

Introduction

Strict laws on vehicle emissions and high fuel prices have been leading to changes in vehicle concepts for years. Throughout the automotive industry, there is a clear trend towards e-mobility. In order to compensate for the weight of the battery and increase the driving range, manufacturers are increasingly relying on modern lightweight materials, including advanced high-strength steels (AHSS) such as complex phase (CP) or dual phase (DP) steels to reduce the weight of their vehicles [1]. The mechanical properties of AHSS are controlled by a specific mixture of different hard microstructural components such as retained austenite, ferrite, bainite, martensite and non-metallic precipitates. Thus, it is possible to cover yield strengths and tensile strengths far above those of conventional deep-drawing and low-alloy steels while maintaining a good formability.

In order to optimally utilise the high potential of AHSS for reducing vehicle weight at reasonable costs, a reliable design of forming and crash behaviour of the sheet metal components is required by use of numerical simulation. Therefore, precise modelling of the material behaviour under process conditions is needed. With regard to sheet metal forming, the yield condition, the hardening behaviour and the forming capacity must be included in the modelling. For the description of the forming capacity of sheet metals, the use of forming limit curves (FLC) is state

of the art. A FLC determines strain states that can be withstood by the sheet metal without necking or fracture. However, it is only valid for linear strain paths and a spectrum of strain states between uniaxial and biaxial tension [2]. Due to the shear-dominated material failure of AHSS, the prediction quality of a FLC is not adequate for that. An alternative to the FLC in sheet metal forming simulation are failure models which take the stress state into account. In most failure models, fracture is described by the failure strain as a function of the stress state [3]. Many models already exist for the mathematical description of these failure surfaces for AHSS, such as the Modified Mohr-Coulomb (MMC) failure model [4]. In order to characterise the material failure, material tests such as uniaxial tensile tests with different notches or holes, shear tests and Nakajima tests are performed to investigate the failure under different stress states from compression to shear to tension. Multiple tests are necessary to describe the material failure realistically in a wide range of different loadings and to parametrise the parameters of the failure model [4]. Those failure characterisation tests are often monitored with an optical measurement system, which is used to determine the fracture initiation on the specimen surface and to calculate the plastic strain. To improve the accuracy of the failure characterisation, a method capable of detecting a critical fracture initiation inside the specimen that remains invisible to the optical measurement system can be used [5]. Furthermore, sometimes the fracture initiation on the specimen surface is hardly to determine optically due to the stress state or because of the stochastic pattern applied on the specimen surface. In this context, acoustic emission (AE) analysis has a high potential for an improvement in failure characterisation due to enhanced fracture detection [6].

Therefore, in this paper an existing testing rig for butterfly specimen with optical measurement system is extended with an acoustical measurement system. Seven loading angles of the butterfly tests, generating seven different stress states, are investigated for two AHSS. The tests are monitored with an optical as well as an acoustical measurement system. Finally, the failure initiation is determined and compared by the three different evaluation methods mechanical, optical as well as acoustical.

Material Characterisation with Acoustic Emission

AE analyses were used prior in the literature to characterise different material properties of metals. Shen et al. investigated the behaviour of titanium during a tensile test with a broadband and a resonant sensor [7]. The yielding and fracture of the material was characterised by a larger amplitude and a higher number of counts exceeding a threshold value. In contrast to the broadband sensor, the resonant sensor was also able to identify necking due to a higher amplitude. AE signals during plastic deformation of a low-carbon steel were analysed by Muravev et al. [8]. The localisation of acoustic emissions in combination with speckle interferometry enabled tracking of the movement of Lüders bands at yielding. Furthermore, it was possible to predict necking and fracture. In [9], Chuluunbat et al. used AE to analyse the fracture behaviour of the steel X70 during tensile tests with notched specimens. The fracture development was recorded simultaneously with a high-speed camera. At the time of fracture development inside the specimen, the AE activity increased rapidly. Changes of the process parameters temperature and strain rate also influenced the AE activity. Panasiuk et al. used the acoustic emission method and Kolmogorov-Sinai entropy to successfully determine the yield point of the aluminium alloy EN AW-7020 during tensile testing [10]. A new acoustic emission activity detection method based on short-term waveform features was invented by Piñal-Moctezuma et al. and applied to tensile tests of sheet metal [11]. In [12], Petit et al. observed the strain localisation features and mechanisms during tensile tests of C35 by coupling AE analysis and electronic speckle pattern interferometry. The AE behaviour of DP steels with different martensite contents was investigated with tensile tests by Khamedi et al. [13]. It was shown that for DP steels with a low martensite content, the damage mechanism was dominated by decohesion of ferrite and martensite. In specimens with a high martensite content, fractures also occurred in the martensite. The different damage mechanisms had a characteristic

frequency range that could be identified by wavelet analysis. Pathak et al. investigated the influence of the stress state on micro-void nucleation for a CP800 and a DP780 using 3D micro-tomography for interrupted tests and in situ digital image correlation during testing [14]. For both steels, little void nucleation was observed under shear deformation but extensive void damage was observed under biaxial tension.

Materials and Methods

The investigated AHSS HCT780C (CP800) with 1.6 mm sheet thickness and HCT980X (DP1000) with 1.5 mm sheet thickness are provided from voestalpine Stahl GmbH. The CP800 is a complex phase steel consisting of martensite, bainite as well as ferrite and the DP1000 is a dual phase steel consisting of martensite as well as ferrite. To investigate the failure behaviour of the steels CP800 and DP1000, butterfly tests are conducted, which are detailed described by Behrens et al. in [15]. The experimental set-up is shown in Fig. 1 and consists of a rotatable testing rig, which is installed in the tensile testing machine S100/ZD from DYNA-MESS Prüfsysteme GmbH.

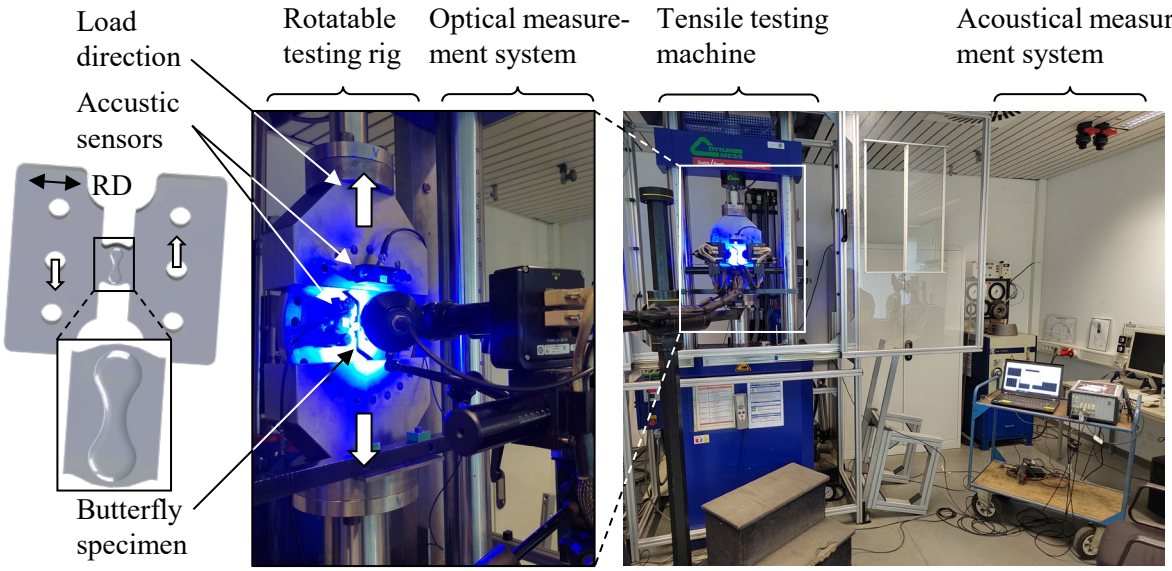

Fig 1: Experimental set-up for butterfly tests with optical and acoustical measurement systems

It further contains the optical measurement system Aramis from Carl Zeiss GOM Metrology GmbH and the acoustical measurement system AMSY-6 from Vallen Systeme GmbH. Piezoelectric sensors of the same company as the measuring system are used to record the acoustic emissions. To receive the signals off the specimen, a resonance sensor (VS900-RIC) and a broadband sensor (AE2045) are used, which are both applied on the rotatable testing rig. Thus, a frequency band of 100-2200 kHz can be investigated. Furthermore, a guard sensor (VS900-RIC) is attached to the tensile test machine as well to record and filter the machine-induced noise. In the following, the resonance sensor will be referred to as AE1 and the broadband sensor as AE2. When applying the AE sensors, the coupling agent Echotrace from Karl Deutsch Prüf- und Messgerätebau GmbH is used. With the rotatable testing rig, the butterfly specimen can be aligned at -3°, 12.5°, 28°, 43.5°, 59°, 74.5° and 90° to the loading direction, which results in different stress states in the centre of the specimen ranging from shear loading to uniaxial tension. During the experiments, the testing rig is fixed against rotation. The seven angles are tested until failure with a velocity of 0.02 mm/s (quasi-static) for both AHSS at room temperature and each test is repeated five times for statistical validity. While testing, the forming force is measured by the tensile testing machine, the displacement of the specimen by the optical measurement system and the acoustic

emission by the acoustical measurement system. The recording frequency of the optical measurement system was 20 Hz and the sound emissions are recorded event-triggered with a sampling rate of 5 MHz.

Each specimen failure is evaluated based on the three methods mechanical, optical and acoustical, as shown in Fig. 2. The mechanical method assumed the failure for each specimen, when a 30 % drop of the forming force appeared in about 0.5 s. The threshold value was chosen based on the inertia of the tensile testing machine. Using the optical method, the fracture initiation on the specimen surface is determined by the images from the optical measurement system. The acoustical signals are characterised on the basis of the form of the signal and their parameters. At the failure initiation, only burst signals (clearly recognisable beginning and end) are obtained. These are first classified based on the amplitude reached. Other certain features such as time and frequency are extracted from the signals and those suitable for differentiation are determined. These included rise-time and the centre of gravity of the frequency spectrum (FCOG). The three methods are compared regarding the failure initiation by evaluating the displacement and plastic strain before fracture determined by each method.

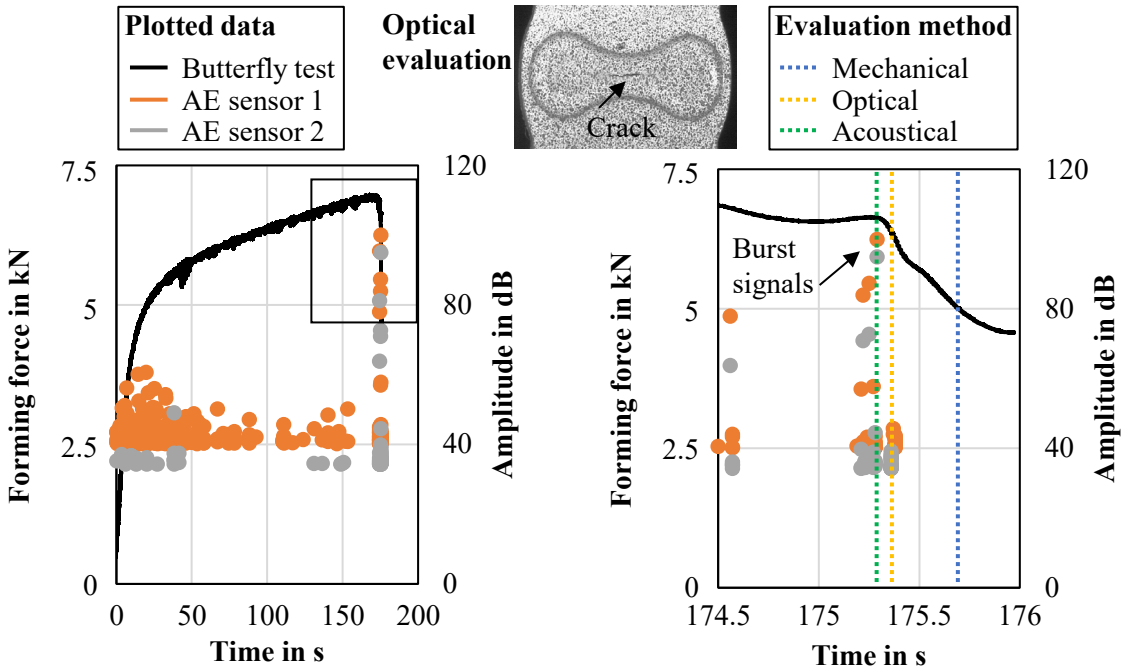

Fig 2: Mechanical, optical and acoustical evaluation methods of material failure

Experimental Results and Comparison of the Evaluation Methods

Fig. 3 displays the forming force-time curve of the performed butterfly tests for CP800 on the left and DP1000 on the right under variation of the loading angle from -3° to 90°. For both materials, the maximum forming force is the highest at a loading angle of 90° and reduces continuously until a loading angle of 12.5°. The reason for this effect is that at a loading angle of 90° the stress state in the specimen is uniaxial tension, which is more and more superimposed with shear loading reducing the loading angle until mostly shear loading is present at -3°. The forming force at -3° is at the same level as 12.5°, but the material failure occurs later. Comparing the CP800 and the DP1000, the maximum forming force for the DP1000 is higher than for the CP800 at every loading angle due to the higher strength of the DP1000.

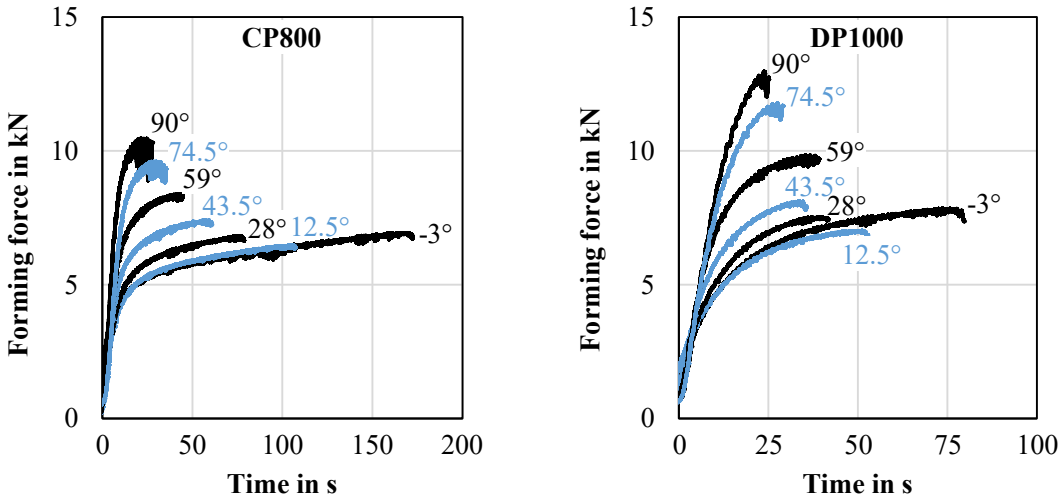

Fig 3: Forming force-time curves of the butterfly specimen for CP800 (left) and DP1000 (right)

The optical measured and calculated plastic strain of the butterfly tests before failure is shown in Fig. 4. At the top, the plastic strain distribution according to von Mises is plotted for CP800 and on the bottom for DP1000 for the seven loading angles determined by the optical evaluation method. As clearly visible at every loading angle for both materials, the plastic strain concentrates on the middle area of the specimen due to the reduced thickness in the specimen centre. Hence, no fractures appeared along the edges of the specimen. In contrast to the maximum forming force, the maximum plastic strain decreases for higher loading angles for both materials. Due to the higher formability of CP800 compared to DP1000, the achieved plastic strain is higher for CP800 at every loading angle.

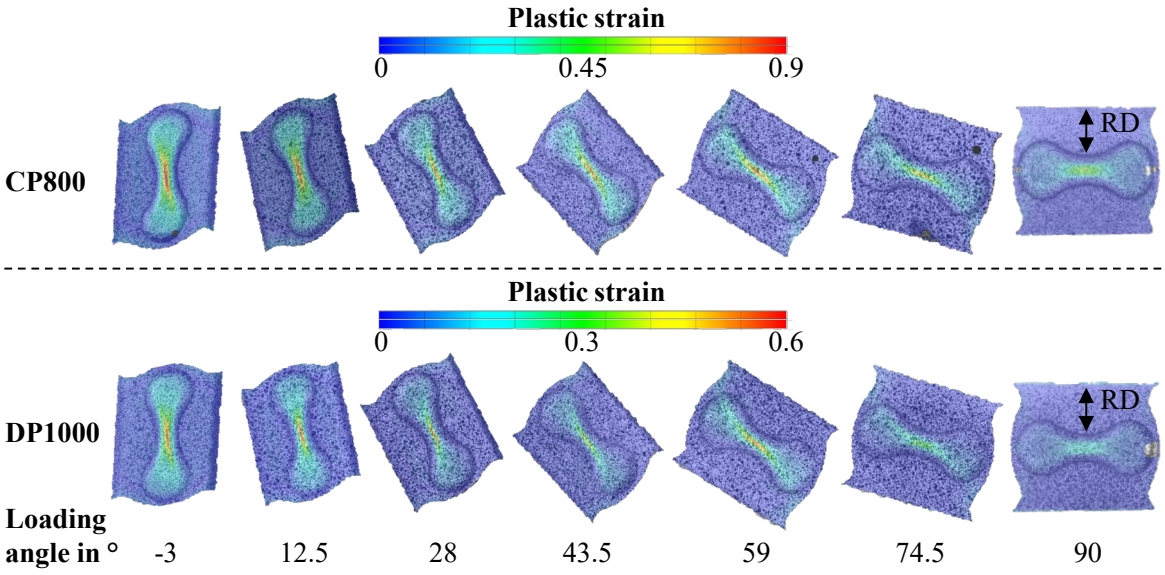

Fig 4: Plastic strain distribution before failure from the optical measurements for CP800 (top) and DP1000 (bottom)

To investigate the influence of the evaluation methods on the results of the butterfly tests, the displacement in load direction and the plastic strain in the centre of the specimen before failure averaged from the five experiments are shown with standard deviation at the top of Fig. 5 for CP800. As to be expected, the displacement before failure is the highest using the mechanical evaluation method and is reduced with the optical evaluation method. The acoustical evaluation

method determines slightly lower or almost the same displacements compared to the mechanical evaluation method, except for the loading angle -3°. Analysing the plastic strain, the effect of the different displacements can be seen well. Although the displacement from the mechanical evaluation method is only slightly higher than from the other methods, the plastic strains determined by the mechanical evaluation method significantly exceed the plastic strains from the other methods for all loading angles.

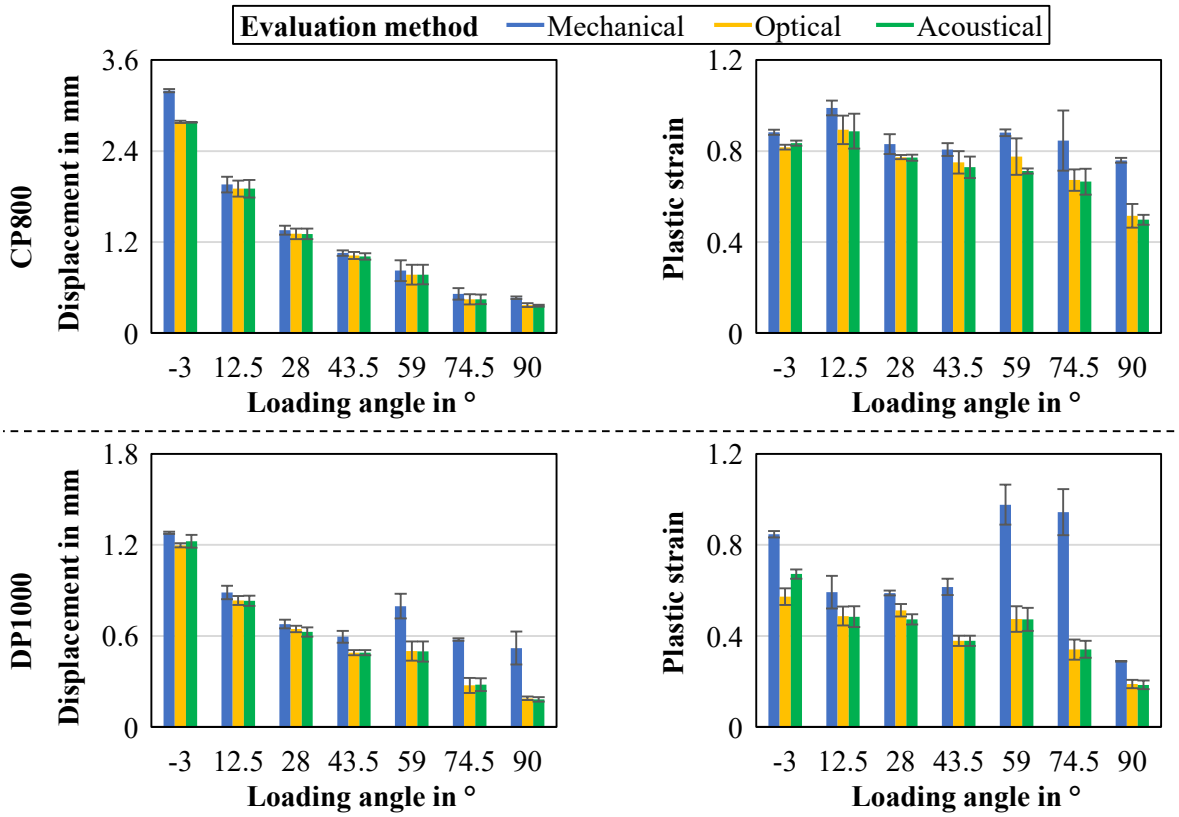

Fig 5: Displacement before failure as well as plastic strain for CP800 (top) and DP1000 (bottom)

Comparing the optical and the acoustical evaluation method, the acoustical evaluation method shows slightly lower values than the optical method likewise to the displacements. Only for a loading angle of -3° the plastic strain of the acoustical evaluation method is higher than the plastic strain of the optical evaluation method. Apparently, the begin of failure under shear loading does not produce an AE signal, which could be measured as well as distinguished from machine-induced noise with the used sensors and amplifiers. The measured AE signals appear after the fracture can already be seen on the specimen surface and propagates in the material. This effect is due to the failure mode of this specific stress state: at the loading angle -3°, a shear stress state and shear failure are present. For the other loading angles, the tension stress state is dominant, which leads to normal failure initiated by the formation and growth of voids. A similar behaviour can be seen for DP1000 at the bottom of Fig. 5. Here the plastic strain before failure using the mechanical evaluation method is often significantly higher than the values determined by the other two methods. Especially for the loading angles 59° and 74.5° of DP1000 the plastic strain before failure of the mechanical evaluation method is much higher than for the other two methods. This is attributed to the fact that the high strength of the DP1000 causes an abrupt failure of the material, especially for the tension stress states at the loading angles 59° and 74.5°.

Summary and Outlook

To increase the determination accuracy of the failure initiation and hence the prediction accuracy of failure models, a test rig for butterfly specimen with optical and an acoustical measurement system was developed. The measurement setup was used to determine the failure initiation of two AHSS under different stress states induced in butterfly specimens by different loading angles using the rotatable butterfly test rig. The failure of the respective specimens was evaluated using optical and acoustical measurements. As a reference, the mechanical failure was determined based on a sudden decrease in the forming force. First, the influence of the loading angle on the required forming force and strain was determined. For low angles, a low load capacity and a high maximum plastic strain according to von Mises were recorded. As the loading angle increases, the load increases and the maximum plastic strain decreases. Subsequently, the time of failure initiation determined by the different measurement methods was compared. The optical and acoustical signals lead to earlier detection of the failure initiation compared to the mechanical signal. However, the acoustical signal can only achieve a small improvement in the determined failure time compared to the optical signal. In the case of a shear stress at -3°, the time of failure determined by means of the acoustical signal was even later than the optical measurement.

In further investigations, an improved recording of the failure initiation in the specimens is to be achieved by replacing the AE measurement amplifier. With a different amplification it is possible to detect signals with higher amplitudes. In addition, a coupling of the measuring systems and the test rig is planned so that the test is interrupted at an early stage with the aid of an automatic failure criterion. Furthermore, the experiments will be numerically modelled and the stress state will be determined for each evaluation method. Failure models like the MMC model will be calibrated based on the results. It is assumed that the failure models for the different methods vary significantly due to a difference in the stress state at the specimen surface and in the specimen centre. Thus, failure models with higher accuracy can be created to represent processes more precisely in the numerical simulation.

Acknowledgment

The authors gratefully acknowledge the support of the German Research Foundation (Deutsche Forschungsgemeinschaft, DFG) within the Project 385276585 ‘‘Improving the failure characterisation of advanced high-strength steel sheets by coupling measurement systems for optical forming analysis with acoustic emission technology’’.

References

[1] N. Fonstein, Dual-phase steels, in: Automotive steels - Design, Metallurgy, Processing and Applications, Elsevier, 2017, pp. 169–216.

[2] B.-A. Behrens, D. Rosenbusch, H. Wester, E. Stockburger, Material Characterization and Modeling for Finite Element Simulation of Press Hardening with AISI 420C, J. of Materi Eng and Perform 31 (2022) 825–832. https://doi.org/10.1007/s11665-021-06216-y

[3] B.-A. Behrens, K. Dröder, A. Hürkamp, M. Droß, H. Wester, E. Stockburger, Finite Element and Finite Volume Modelling of Friction Drilling HSLA Steel under Experimental Comparison, Materials 14 (2021). https://doi.org/10.3390/ma14205997

[4] Y. Bai, T. Wierzbicki, Application of extended Mohr–Coulomb criterion to ductile fracture, Int J Fract 161 (2010) 1–20. https://doi.org/10.1007/s10704-009-9422-8

[5] E. Martinez-Gonzalez, I. Picas, D. Casellas, J. Romeu, Detection of crack nucleation and growth in tool steels using fracture tests and acoustic emission, Meccanica 50 (2015) 1155–1166. https://doi.org/10.1007/s11012-013-9858-9

[6] B.-A. Behrens, S. Hübner, K. Wölki, Acoustic Emission – A promising and challenging technique for process monitoring in sheet metal forming, in: Journal of Manufacturin Processes, Volume 29, 2017, pp. 281–288. https://doi.org/10.1016/j.jmapro.2017.08.002

[7] G. Shen, L. Li, Z. Zhang, Z. Wu, Acoustic Emission Behavior of Titanium During Tensile Deformation, in: Advances in Acoustic Emission Technology, Springer, 2015, pp. 235–243. https://doi.org/10.1007/978-1-4939-1239-1_22

[8] T.V. Murav'ev, L.B. Zuev, Acoustic emission during the development of a Lüders band in a low-carbon steel, Tech. Phys. 53 (2008) 1094–1098. https://doi.org/10.1134/S1063784208080203

[9] T. Chuluunbat, C. Lu, A. Kostryzhev, K. Tieu, Investigation of X70 line pipe steel fracture during single edge-notched tensile testing using acoustic emission monitoring, Mater. Sci. Eng. A 640 (2015) 471–479. https://doi.org/10.1016/j.msea.2015.06.030

[10] K. Panasiuk, L. Kyziol, K. Dudzik, G. Hajdukiewicz, Application of the Acoustic Emission Method and Kolmogorov-Sinai Metric Entropy in Determining the Yield Point in Aluminium Alloy, Materials 13 (2020). https://doi.org/10.3390/ma13061386

[11] F. Piñal-Moctezuma, M. Delgado-Prieto, L. Romeral-Martínez, An acoustic emission activity detection method based on short-term waveform features: Application to metallic components under uniaxial tensile test, Mechanical Systems and Signal Processing 142 (2020) 106753. https://doi.org/10.1016/j.ymssp.2020.106753

[12] J. Petit, G. Montay, M. François, Strain Localization in Mild (Low Carbon) Steel Observed by Acoustic Emission - ESPI Coupling during Tensile Test, Exp Mech 58 (2018) 743–758. https://doi.org/10.1007/s11340-018-0379-2

[13] R. Khamedi, A. Fallahi, A. Refahi Oskouei, Effect of martensite phase volume fraction on acoustic emission signals using wavelet packet analysis during tensile loading of dual phase steels, Materials & Design 31 (2010) 2752–2759. https://doi.org/10.1016/j.matdes.2010.01.019

[14] N. Pathak, J. Adrien, C. Butcher, E. Maire, M. Worswick, Experimental stress state-dependent void nucleation behavior for advanced high strength steels, Int. J. Mech. Sci. 179 (2020) 105661. https://doi.org/10.1016/j.ijmecsci.2020.105661

[15] B.-A. Behrens, D. Rosenbusch, H. Wester, P. Althaus, Comparison of three different ductile damage models for deep drawing simulation of high-strength steels, IOP Conf. Ser.: Mater. Sci. Eng. 1238 (2022) 12021. https://doi.org/10.1088/1757-899X/1238/1/012021